

UNCLASSIFIED

AD 404 711

DEFENSE DOCUMENTATION CENTER

FOR

SCIENTIFIC AND TECHNICAL INFORMATION

CAMERON STATION, ALEXANDRIA, VIRGINIA



UNCLASSIFIED

NOTICE: When government or other drawings, specifications or other data are used for any purpose other than in connection with a definitely related government procurement operation, the U. S. Government thereby incurs no responsibility, nor any obligation whatsoever; and the fact that the Government may have formulated, furnished, or in any way supplied the said drawings, specifications, or other data is not to be regarded by implication or otherwise as in any manner licensing the holder or any other person or corporation, or conveying any rights or permission to manufacture, use or sell any patented invention that may in any way be related thereto.

AD No. 404711
ASTIA FILE COPY

404 711

④
\$ 3.60

PETER GRIFFITH

January 1963

~~Report No. 7-7673-23~~

Department of Mechanical
Engineering
Massachusetts Institute
of Technology

DDC

MAY 21 1963

TISIA A

ENGINEERING PROJECTS LABORATORY
ENGINEERING PROJECTS LABORATOR'
ENGINEERING PROJECTS LABORATO'
ENGINEERING PROJECTS LABORAT'
ENGINEERING PROJECTS LABORA'
ENGINEERING PROJECTS LABOR
ENGINEERING PROJECTS LABO'
ENGINEERING PROJECTS LAB
ENGINEERING PROJECTS LA
ENGINEERING PROJECTS L
ENGINEERING PROJECTS
ENGINEERING PROJECT
ENGINEERING
ENGINEERING

14
TECHNICAL REPORT NO. 23

7673 23

⑥ The Prediction of Low Quality Boiling Voids

⑩ by

Peter Griffith*

⑦ thru ⑨ NA

For

Office of Naval Research

⑮ Contract NONR-1841-939

DSR No. 7-7673

⑪ January 1963

⑫ 26 p

⑬ NA

Division of Sponsored Research

⑤ 555 000 Massachusetts Institute of Technology

Cambridge 39, Massachusetts

⑮ thru ⑲ NA


⑳ 71

㉑ NA


* Associate Professor of Mechanical Engineering
Massachusetts Institute of Technology

opc

ABSTRACT



Slug flow theory is used to predict the density in heated channels of various shapes. In order to make this calculation possible, measurements are made of the bubble-rise velocity in annuli, tube bundles, and channels. It is found that the large dimension is most important in channels, and the shroud dimension most important in annuli and tube bundles. It is also found that no rotationally symmetrical bubble shapes are obtained in annuli and tube bundles. Finally, a comparison is made between the theory, which contains no free constants, and the experiments. The comparison is good. The results, as presented, apply only to vertical, heated channels of various shapes with up-flow in the low quality region.



Introduction

Boiling void data are difficult to obtain and very difficult to predict. Because of this it is important to make effective use of all existing data in order to make predictions for other geometries, pressures and velocities. In this work, the effects of throughput velocity, channel size, geometry, and fluid quality are all considered and combined into a rational, unified correlation scheme. The basis of this work is an expression for slug flow density developed in an earlier paper (1). The results, therefore, apply only to the slug flow, flow regime which means very high velocities, high qualities and high heat fluxes are not covered by the methods suggested in this work. The exact limits on velocity, quality and heat flux are not known at this time as our knowledge of the flow regime boundaries at elevated pressure is still too limited. However, the limits where this correlation has been found to work will be presented along with a mention of those data which fell outside the limits.

Evidence that slug flow exists in heated channels is skimpy at this time as visual observation are so difficult to make at elevated pressure. However, three different references refer to slug flow in three different geometries and their comments will be listed. Reference (2) notes in passing that, in an annulus with boiling freon, a slug flow flow regime was passed through. Reference (3) says that slug and a sluggish flow existed from qualities between 0 and 30% at a mass velocity of 100 lb/sec ft^2 and a heat flux of about $0.9 \times 10^6 \text{ Btu/hr ft}^2$. The channel was 0.25" or 0.5" by 2.1". Higher mass velocities and generally higher heat fluxes did not yield any slug flow in these experiments. The third reference showing that

slug flow exists in heated channels is reported in reference (4). In this reference, gamma ray void measurements were made on a channel 1.11 cm x 4.44 cm. The source strength was very high so that short counting times were needed to get a representative sample from which the density could be computed. In these experiments the velocity into the test section was 77 cm/sec. The pressure was about 400 psia and the heat transfer rate 67,000 Btu/hr ft². As this reference is not generally distributed it will be quoted from directly.

"Fairly regular signal variations, with frequencies in the order of 20 to 30 cycles per second, were always seen near the exit. At an average void amplitude of 50%, for instance, the variations could correspond to void changes as large as $\pm 20\%$."

These three observations summarize the direct evidence that slug flow does exist in heated channels at elevated pressure.

In this paper, the theoretical framework for the correlation scheme will be presented, then the measurements of bubble rise velocity in channels of various shapes will be given and finally the correlation scheme which has been developed will be compared with void data already in the literature.

Slug Flow Void Fraction, Density, and Velocity Ratio

References (1) and (5) develop expressions for the void fraction in slug flow. The development of the relevant equation will not be repeated here but only the results presented. The primary result is

$$R_s = \frac{Q_g}{Q_f + Q_g + V_b A} \quad (1)$$

The only unknown in this equation is the bubble rise velocity. This will be determined in a later section. With the void fraction given in equation (1)

**THIS
PAGE
IS
MISSING
IN
ORIGINAL
DOCUMENT**

The Constant K_1

The velocity V_b , physically, is the velocity of the slug flow bubbles with respect to the liquid ahead of them. In a tube initially filled with liquid and closed at the top, it is the velocity which one would see the bubble rise when the tube is emptied. In general, this velocity is a function of gravity, inertia, surface and viscous forces. For the larger tubes and channels of interest, the gravity and inertia forces predominate and a very simple expression for the bubble rise velocity is obtained. For the tube emptying experiment, this expression is

$$\frac{V_b}{\sqrt{g D_b}} = K_1 \quad (7)$$

The constant K_1 differs for different geometries and has been determined experimentally for the various test sections of interest. In two particular cases, it has been computed from potential flow theory, the round tube with the references reported in (1) or (5) and for channels (6). A complete presentation of the constant K_1 for all tube sizes and all fluid properties is given in reference (7).^{*} For all the data presented here viscous forces are shown to be negligible and surface forces are quite small because of the large size channels used. K_1 is, therefore, a real constant.

^{*}In Reference (1) a curve of K_1 is given as a function of Reynolds number. Actually surface forces are more important in those experiments. Therefore, the more general presentation of reference (7) is to be preferred for determining K_1 where viscous and capillary forces are important. For all the data presented here they are secondary.

The experiments used to determine K_1 were run in several test sections using water and a water-glycerine mixture and glycerine. The test sections were hung vertically and filled from a container of liquid by drawing up through the bottom. When filling was complete, the top was plugged and the motion picture camera started. The liquid bath at the bottom was dropped and the tube emptied. The rise velocity was recorded on the motion picture film. The time it took to traverse a known distance was determined by a frame by frame examination of the film. Identical test sections were tried with the three test fluids, water, 25% by weight glycerine, and pure glycerine. A summary of the test section dimensions is presented below in Table I.

TABLE I

<u>Test Section</u>	<u>Shape</u>	<u>Dimensions</u>			
		<u>D_b</u>	<u>D_s</u>	<u>L</u>	
A	Rectangle	2.05"	2.03"	23.75"	
B	"	1.98"	1.48"	23.75"	
C	"	1.49"	.35"	23.75"	
D	"	1.78"	.13"	23.75"	
E	"	5.25"	.435"	23.75"	
		<u>D_b</u>	<u>D_i</u>	<u>L</u>	
F	Annulus	2.00	.233"	48"	
G	"	2.00	.485"	48"	
H	"	2.00	.70"	48"	
		<u>D_b</u>	<u>D_t</u>	<u>D_c</u>	<u>L</u>
I	7 Tube, Tube Bundle	2.00	.152"	1.18"	48"
J	"	2.00	.260"	1.18"	48"
K	"	2.00	.393"	1.18"	48"

As a check on the whole procedure the rise velocity was determined in the 2" round tube without any insert. K_1 turned out to be 0.34 which is 3% low. Most of this error is probably tied in with the timing and measuring from the motion picture film. Therefore, the results presented in Figure (1) are accurate to about 3%.

A number of unexpected results were obtained from these experiments. First, (and according to the predictions of reference (6) also) the large rather than the small dimension is the significant one in channels. It was observed in channels that almost all the liquid runs down the two small walls. Were a hydraulic diameter notion used to obtain a dimension for substituting in equation (7) it would be seriously in error. Apparently, as a consequence of this fact the annuli and tube bundles also behaved quite differently from what one would expect. Though both geometries have a certain kind of symmetry, no symmetrical bubbles were obtained. The bubble would move over to the side and stay there. Which side it would rise on was quite random, but it never assumed a nice, rotationally symmetrical shape as it does in a round tube.

This fact is compatible with our observations in channels, if one regards an annulus, in the limit, as a channel wrapped around on itself. There is a tail by the bubble down which the liquid falls. This same fact leads to an increase in bubble rise velocity at a fixed shroud diameter with increasing inner rod diameter as the relevant dimension approaches the shroud circumference. This occurs even though the hydraulic diameter is decreasing. Along the same vein, the tube bundles with the largest tubes show the largest bubble rise velocities. In this case there is also a marked channeling with three or four of the passages between tubes consisting almost entirely of gas while the rest consist almost entirely of liquid. In these experiments no particular

passage seemed favored.

Measurements were run in a very small channel (D of Table 1) and the constant K_1 was slightly below what was predicted in reference (6), 0.23 ± 0.02 . In this case the small dimension of the channel was so small, surface forces kept any liquid from running down the large flat faces of the channel.

In calculating the various constants K_1 for figure (1) the most important dimension was used. When cross plotting figure (1) to get figure (2), the other dimension is taken care of in the geometric parameter. Figure (2) does not have the results for channel D plotted as the surface forces were clearly not negligible for this experiment. The Reynolds number of figure (1) is based on the hydraulic diameter as that is normally the relevant dimension for scaling the ratio viscous to inertia forces.

The geometric parameter of figure (2) is defined so as to always have a value between zero and one. The dotted lines of figure (2) are extrapolations to values one would anticipate from the limit that particular geometry approaches. For instance, the annuli and tube bundles approach the pipe for vanishingly small inserts while the annulus approaches a channel of large dimension (πD_o). Naturally tube bundles, which have more than one geometric parameter, will not all fall on exactly the same curve which is given here. These measurements were made on one particular set of bundles and do provide an estimate for almost any bundle. This estimate is probably quite good because the shroud diameter is more important than any of the internal dimensions. The tube bundle curve has not been extrapolated to the right as it rises so steeply and one does not know what limit it is approaching.

One experimental point from reference (6) has been plotted on figure (2) and is for a rectangular channel 1" x 4.07" in cross section. It is slightly above the cross plot for the channels of these experiments. The accuracy of the measurement of reference (6) was ± 0.02 for $K_1 = 0.29$.

The Constant K_2

Reference (5) reports a correlation for V_b in a round pipe which allows one to easily interpret the significance of K_2 and calculate its value for other geometries. They found in turbulent flow that with respect to the liquid ahead, a bubble moves with a velocity equal to

$$V_b = .2 \left(\frac{Q_c + Q_d}{A} \right) + .35 \sqrt{g D} \quad (8)$$

The 0.35 is K_1 while the coefficient 0.2 is K_2 . It has the following significance. It is the proportion that the core of liquid in the center the pipe moves faster than the mean velocity in the pipe. For a throughput Reynolds number greater than 8000, reference (5) found K_2 was virtually independent of Reynolds number. This is to be expected as the ratio of the mean to centerline velocity in this region is only a very weak function of Reynolds number. For Reynolds numbers less than 8000, no simple interpretation of this coefficient is possible and it is recommended that the methods of reference (1) be used in this region. The curves of K_2 (figure 3) were computed assuming that

$$K_2 = \frac{V_m - V_{av}}{V_{av}} \quad (9)$$

and that the value for this ratio was constant for turbulent flow. The details of the calculation are as follows

The value of the coefficient K_2 of 0.2 from reference (5) is slightly less than the ratio one would compute from equation (9) for the Reynolds numbers that were actually run. For this reason a slightly unconventional power for the velocity profile law was chosen in order that the result of the integration yielding K_2 from equation (9) be the 0.2 that was actually observed. V for equation (9) was obtained by integrating out from the wall using

$$V = V_m \left(\frac{r_m - r}{r_m} \right)^{\frac{1}{n}} \quad (10)$$

$$n = 7.8 \quad (11)$$

$$V_{av} = \frac{1}{A} \int_0^A V dA \quad (12)$$

The set of equations (9), (10), (11) and (12) are sufficient for infinite flat plates and tubes. For annuli additional information was needed.

For infinite flat plates V_m must be at the center by symmetry. For annuli the location of V_m was determined by putting the momentum equation on a section from the rod to the V_m position and from the shroud to the V_m position. The pressure gradients for these two control volumes were then equated. This yields equation (13).

$$\left(\frac{\gamma_o}{\gamma_i} \right) \frac{R_o}{R_i} = \frac{R_o^2 - R_m^2}{R_m^2 - R_i^2} \quad (13)$$

The ratio γ_o / γ_i was obtained by consideration of the universal velocity profile and the requirement that the velocity coming in from each wall to the V_m point be the same. When these velocities were equated the result was

$$\begin{aligned} & \left(\frac{\gamma_o}{\rho} \right)^{1/2} \left[5.5 + 2.5 \ln \left(\frac{R_o - R_m}{\nu} \right) \left(\frac{\gamma_o}{\rho} \right)^{1/2} \right] \\ & = \left(\frac{\gamma_i}{\rho} \right)^{1/2} \left[5.5 + 2.5 \ln \left(\frac{R_m - R_i}{\nu} \right) \left(\frac{\gamma_i}{\rho} \right)^{1/2} \right] \quad (14) \end{aligned}$$

(See reference (18)).

Equations (13) and (14) were then solved in the following manner. A particular geometry and fluid were picked and a Reynolds number chosen, in

this case 360,000, to conform to the value for " η " given in equation (11). The mean wall shear stress was evaluated from the hydraulic diameter notion and equations (13) and (14) solved by trial and error. In each case it was required that the mean wall shear stress be the weighted average of τ_i and τ_o . For a given Reynolds number and R_i/R_o , the value of R_m/R_i is invariant so the actual channel size and fluid properties chosen to evaluate τ do not matter. After all this effort it was found that for annuli of the interesting diameter ratios, the shear stresses on the shroud and insert were virtually equal. The location of r_m was obtained from equations (13) and (14) and then the mean velocity was obtained from (10), (11) and (12). For tube bundles it was assumed that K_2 would have the same value as it would in an annulus of the same hydraulic to shroud diameter ratio. This is plausible but cannot be proven.

There are three points on the curve for channels. One is the large aspect ratio limit which is the same as for infinite flat plates. The other two points were obtained by a graphical integration of the plots in reference (8) for a square duct and a rectangular duct of 3.5 aspect ratio. The Reynolds numbers for these experiments were about 40,000. Though this mixture of calculation and experiment is esthetically not pleasing the actual result is undoubtedly better than either method used alone.

The Constant K_3

In reference (9) it was shown that in an unheated entrance region the slug flow bubbles are influenced by the bubbles ahead and rise more rapidly. In a sense the bubbles in a boiling channel are also in an entrance region. Bubbles in a heated section are formed at the wall, grow, become close enough

to affect each other, catch up and agglomerate. The net result of these processes is an augmented bubble rise velocity. In order to take cognizance of this effect, K_3 has been defined. Originally, it was expected that it would be a function of heat flux. When a look was taken at the data however, no such effect emerged. Therefore, the best constant value was chosen by an examination of the data. It is, for^a section with heat addition

$$K_3 = 1.6 \quad (15)$$

By definition, for fully developed slug flow without heat addition

$$K_3 = 1 \quad (16)$$

This completes the discussion of the significance of constants in equation (6).

The Comparison with the Data

Equations (1) or (5), (6) and (15) along with figures (2) and (3) suffice to allow one to make a comparison between the calculated and measured voids from the literature. Before that is done however, it is appropriate to say a few words about the flow regime.

Basically, there appear to be three flow regimes in the quality region, bubbly, slug and annular. The dividing lines between these regimes are not known with any certainty but we do have some evidence as to where the boundaries lie and what affects their position.

The bubbly-slug transition lies at an R_g of about 10% for very pure water at low velocity and somewhere between 10 and 30% for water of tap water purity (10). (Of course, for water with soap in it the bubbles can persist to much higher concentrations.) At very high velocity a frothy or

misty mixture of liquid and vapor is to be expected. For bubbly flow the bubbles move rather slowly with respect to the liquid and the slip is much lower than for slug flow (11). Also the slip tends to decrease with increasing quality (at constant mass velocity) rather than increase as it does in slug flow. We should expect then, that the slip velocity ratio would be overestimated and the density underestimated, by the slug flow expressions at the very lowest quality points.

The transition from slug to annular flow appears to take place at the point where the vapor shear stress pulls the liquid film, which is on the wall, up with it. The vapor shear stress depends on vapor density so one would expect this boundary to be sensitive to system pressure. We should look for a systematic deviation from the slug flow void predictions at high velocity and pressure with the void fraction being higher than predicted. At very high velocity a limiting void fraction is obtained from equation (1) and (6).

This is

$$R_g \rightarrow \frac{1}{1 + K_2} \quad (17)$$

Any measured void fraction which is greater than this asymptote cannot be predicted from slug flow theory. For such voids the flow regime must be either annular or spray.

It is felt that if one were to look inside the test sections in which the data, which has been correlated, was taken, one would see a churning turbulent mixture with a few large bubbles near the middle and a large number of small bubbles in the wakes of the large ones. Most of the vapor transport would occur in the large bubbles. As only one quantity, V_b , affects R_g in equation

(1) the details of the flow configuration do not matter. The important thing is that all the vapor moves with the same velocity, V_b . The flow regime observations made in references (3) and (4) support this general picture.

All the data correlated expresses the condition of the material passing a point in terms of an inlet velocity and the quality at the point in question. To get the Q_f and Q_g which are needed to substitute in equations (1), (5), and (6) it is necessary to use continuity and a heat balance. The resulting equations are (for constant area)

$$Q_f = A V_i (1-x) (\rho_i / \rho_f) \quad (18)$$

$$Q_g = A V_i (x) (\rho_i / \rho_g) \quad (19)$$

We shall now proceed to an examination of the data experimenter by experimenter.

The Data of Haywood

Haywood et al (12) measured the density in two vertical 1.5" bore heated pipes, 16 and 24 long. There was no evidence of any difference between the performance of the long and the shorter pipe. The heat fluxes were in the range zero to about 80,000 Btu/hr ft². All measurements were made at the exit by traversing the pipe with a gamma ray. There is no indication of any ion exchanger in the loop which was fabricated from mild steel. We might then expect a transition to slug flow at a void fraction of about 30%. The lowest quality points would have a slip velocity ratio very close to one.

In order to evaluate the slip velocity ratios for this data using equations (5), (6), (15), (18), and (19), it was necessary to know what velocity the water came into the test section. Reference (12) did not state this but did give a plot showing the range of inlet Reynolds numbers tested. Working backwards it was found that the inlet velocity ranged from four to six ft/sec. For plotting the curves on figure 4 a constant value of 5 ft/sec was chosen as, for such a high inlet velocity, the slip velocity ratio depends only very slightly on velocity. It was stated in reference (12) that no effect of inlet velocity on slip velocity ratio could be detected.

For these data, the correlation can be considered satisfactory. There is some evidence of a systematic break away to higher slip velocities than the slug flow theory can yield for 250 and 600 psia. This might well be a transition to annular flow. The number of points is too small, however, to form a definite conclusion.

The Data of Christiansen

Reference (4) reports some density measurements made in a 1.11 by 4.44 cm channel at pressures of 400, 600, 800, and 1000 psia. Figure (5) shows the correlation of this data. Not all the data presented were correlated, because the only significant parameter was inlet subcooling. In the quality region it was shown, inlet subcooling did not affect the results so that just the two lowest subcooling runs were correlated. These runs showed the maximum area of interest. The subcooled boiling voids are not predicted for two reasons. The first is, the voids are at the wall rather than in the center so we cannot have slug flow and second a heat balance does not yield an indication of the flowing void. The heat flux in these experiments was 178,000 and

67,000 Btu/hr ft² for figures (5a) and (5b) respectively.

A figure in reference (4) shows that the void concentrates near the center at a void fraction of 20%. As the system is made of stainless steel and is filled anew each day with distilled water, we can confidently expect an immediate transition to slug flow at this void fraction.

Figure (5b) shows a systematic break away from the slug flow theory at the very highest void fraction. If it is assumed there is no slip between the phases, the void for the highest quality point can be predicted quite well. This is an indication that a transition to froth flow might have taken place. The correlation between theory and experiment can be considered quite satisfactory here.

The Data of Marchaterre

Reference (13) reports data taken in a rectangular test section .438" x 3.687" x 48". The test section was really a channel bundle consisting of three channels of the above dimensions and two wall channels with only one side heated. In order to make the comparison shown on figure (6), it was assumed all the channels were the size given above. Equations (5), (6), (15), (18), and (19) were used. The arrows show the approximate location of the 10% void points. The correlation below this can be expected to be poor, both because we cannot reasonably expect to have slug flow and the precision of the void measurement is low. The poor precision is clearly shown in figure (6a) where absurd velocity ratios are obtained for the first few points. Ten per cent is taken as the critical void fraction for the transition to slug flow as an ion exchanger was continuously used in this system. This

means the water was very pure so that an immediate transition to slug flow could be expected. The extreme conditions of pressure and heat flux for these data are presented along with an intermediate run. The heat flux in these experiments ranged up to 79,000 Btu/hr ft².

Data of Reference 14

The test section for this data is almost the same as the preceding being .5" x 3.5" x 60". An immense number of points were reported but only the first 50 were used. The pressure was uniformly at 150 psig with various inlet velocities. The heat flux ranged up to 42,000 Btu/hr ft². These points supplement those of the preceding figure in that the inlet velocity has been varied. In a general way the heat flux tended to stay constant in these experiments so that the highest inlet velocities gave the lowest exit qualities. For this reason the range of exit velocities is nothing like the ten to one range of inlet velocities. All the measurements reported on figure (7) were taken at the exit of the test section where slug flow was sure to exist if it could exist at all.

Though the scatter is bad, there is no systematic deviation with velocity. It is felt that this is all one can expect with these data.

Data of Spigt et al

Reference (15) reports some density data taken in an annulus 33.7 mm ID x 72.0 mm OD x 2400 mm long. Inlet velocity ranges up to 1.35 m/sec and exit quality up to 2.5%. The heat flux in these experiments ranged up to 250,000 Btu/hr ft². As the measurements were all made near the end of the test section at a fixed location almost any void fraction above 10% can be

expected to be in slug flow. Using equations (1), (6), (15), (18), and (19) one can solve for the void fraction as a function of power. (The information given in reference (15) is not sufficient to make this calculation. A personal communication gave the corresponding qualities for the data reported in reference (15).)

An interesting fact emerges from these comparisons. The low pressure run, Figure (8a), gives a poor correlation. It is almost certain this is due to the fact that an equilibrium heat balance is used to obtain flowing voids. If equilibrium is not attained, the flowing voids will be less and the fraction of vapor less than is computed. At high void fraction one would expect the correlation to improve because of the larger interfacial area between the vapor and liquid. This is born out by the experiments. At high pressure, the existence of a little superheat in the liquid makes a far smaller difference in the error in the computed flowing voids so the correlation improves. Figure (8b) shows this.

Discussion

The most important lack in this work, and indeed in the whole field of two phase flow, is the knowledge of the location of the two phase flow, flow regime boundaries. Though there is no evidence that slug flow does not exist, a direct observation of the flow regime for the data used in this work would add a lot to the convincingness of the correlation.

It is appropriate at this time to mention one set of void data that did not fit in the framework of this paper. It is the data reported in reference (16). The test section is .1" x 1" cross section and the pressure 2000 psia. This data does not fit in with any other correlation either, but

the reason why is not obvious. Compared with the bulk of the data correlated, the heat fluxes and pressures are higher and the test section smaller and shorter than any of those correlated. It is felt that the high heat fluxes, .15 to $.5 \times 10^6$ Btu/hr ft², and the shortness of the test section, 27", do not allow slug flow to develop. The slip velocity ratio of almost one, which they observe, is indicative of a froth flow pattern. Again, a better knowledge of the location of the flow regime boundaries would probably show a clear difference between this data and that which correlated.

It would be very nice to be able to predict wall shear stress too. In so far as this work is based on a tangible model, one should be able to use it to predict wall shear stress also. In principal, it can be done, but the complications of determining a characteristic bubble and slug length and then integrating to get a mean wall shear stress are very great, and for most problems probably not worth while. However, reference (17) presents a method that gives very good results for unheated pipes. By using a mean slug length which is compatible with a value of $K_3 = 1.6$, one could go through a similar calculation for the heated channel.

In addition to vertical upflow, this same framework used here could be adapted to inclined test sections if the appropriate values for K_1 were measured. Down flow could be fit in also, though here the bubbles do not rise in the middle of the pipe at all and a new curve K_2 would have to be determined also.

CAPTIONS

Figure 1 - The raw data showing the independence of K_1 on the viscosity of the liquid. The peculiar increase in K_1 associated with the tube bundles in which the liquid is glycerine is due to a pronounced channeling of the liquid. For even lower Reynolds numbers, K_1 must decrease again.

Figure 2 - Cross plot of Figure 1 for large Reynolds number. The point shown on the curve for rectangles is from reference (6) for a rectangle 1" x 4.06" in cross section. They gave the value for K_1 as 0.29 ± 0.02 . Dotted extrapolations are as follows. Annuli and tube bundles approach a tube, of shroud diameter, for very small inserts. Annuli approach a channel of πD_b width for very small clearances as shown on the right. The triangle on the left axis is the potential flow limit from reference (6) which gives K_1 is $.23 \pm .01$.

Figure 3 - K_2 vs. the geometric parameter for various types of sections. The two points on the rectangular section channel are obtained from reference (8) by planimetry. The rest of the curves were obtained by calculation as described in the text. It is assumed, without proof, that the K_2 for tube bundles is the same as the value for annuli of the same hydraulic diameter. For this curve N_{Re} must be greater than 8,000.

Figure 4 - Data of reference (12), with the conditions as follows. Inlet velocity about 5 ft/sec, length is 16 or 24 feet, q/A is up to 80,000 Btu/hr ft² with the test position always fixed at the exit

of the heated section.

- a. $P = 2100$ psia
- b. $P = 1250$ psia
- c. $P = 600$ psia
- d. $P = 250$ psia

Figure 5 - Data of reference 4 taken on a $1.11 \times 4.44 \times 127$ cm rectangular test section with water. These two runs were chosen out of the 16 presented as the length of channel in the quality region was the greatest. Neither inlet subcooling or heat flux appeared to make any difference as long as the void fraction was greater than 20%. The conditions are as follows:

- | | |
|--|---------------------------------------|
| a. $P = 40.8$ ata | b. $P = 27.2$ ata |
| $V_1 = 115$ cm/sec | $V_1 = 77$ cm/sec |
| $q/A = 178,000$ Btu/hr ft ² | $q/A = 67,000$ Btu/hr ft ² |

Figure 6 - Data of reference 13 - channel dimensions $.438'' \times 3.687 \times 48''$.

Out of the immense number of points available, the runs with the highest flux and lowest pressure, the lowest heat flux and highest pressure and the highest heat flux and highest pressure and one intermediate pressure were chosen. The arrows are the approximate location of the 10% void fraction point in the test sections.

The conditions are:

- | | |
|----------------------|----------------------|
| a. $P = 614.46$ psia | b. $P = 114.51$ psia |
| $q = 13.20$ KW/liter | $q = 39.99$ KW/liter |
| $V_1 = 1.52$ ft/sec | $V_1 = 1.70$ ft/sec |
| c. $P = 314.34$ | d. $P = 614.39$ psia |
| $q = 26.40$ KW/liter | $q = 50.24$ KW/liter |
| $V_1 = 1.71$ ft/sec | $V_1 = 1.8$ ft/sec |

Figure 7 - Data of reference 14. Test section is rectangular in cross section and is .5 x 3.5 x 60". Of the immense number of points the first 50 were taken. The conditions were all at 150 psig with various inlet velocities. The extremes are:

$$V_i = 1.18 \text{ ft/sec}$$

$$x_{\text{exit}} = .0423$$

$$V_i = 11.8 \text{ ft/sec}$$

$$x_{\text{exit}} = .00655$$

The points on figure (7) are separated out into three classes:

●	0	<	V_i	<	3 ft/sec
□	3	<	V_i	<	7 ft/sec
×	9	<	V_i	<	12 ft/sec

Figure 8 - The data of reference 16. The inlet velocity goes up to 1.35 m/sec in an annulus 33.7 mm ID and 72.0 mm OD. The fluid again is water while the pressures are:

a. $P = 52.4 \text{ psia}$

b. $P = 145.4 \text{ psia}$

BIBLIOGRAPHY

1. Griffith, P., G. B. Wallis, "Two Phase Slug Flow," J. of Heat Transfer, Vol. 83, p. 307, No. 3, (Series C. Trans. ASME) 1961.
2. Sacks, P. R., A. K. Long, "Correlation for Heat Transfer in Stratified Two-Phase Flow with Vaporization," Int. J. Heat and Mass Transfer, Vol. 2, pp. 122-30, No. 3, April, 1961.
3. Tippets, F. E., "Critical Heat Fluxes and Flow Patterns in High Pressure Boiling Water Flows," ASME Paper No. 62-WA-162.
4. Christiansen, Helge, "Power to Void Transfer Functions," Ph.D. Thesis, Nuclear Engineering, (Chapter XV), M.I.T., September, 1961.
5. Nicklin, D. J., J. O. Wilkes, J. F. Davidson, "Two Phase Flow in Vertical Tubes," Trans. Inst. of Chem. Eng., Vol. 40, p. 61, 1962.
6. Birkhoff, G. and D. Carter, "Rising Plane Bubbles," J. of Rational Mechanics and Analysis, Vol. 6, pp. 769-780, No. 6, November, 1957.
7. Wallis, G. B., "General Correlations for the Rise Velocity of Cylindrical Bubbles in Vertical Tubes," Report No. 62GL130, General Engineering Laboratory, General Electric Co., Schenectady, N. Y., August, 1962.
8. Nikuradse, J., "Geschwindigkeitsverteilung in Stromungen," Forschungsarbeiten auf dem Gebiet des Ingenieur Wesens," Heft 281, 1926.
9. Moissis, R., and P. Griffith, "Entrance Effects in a Two Phase Slug Flow," J. of Heat Transfer, p. 29, February, 1962.
10. Radovich, N. A. and R. Moissis, "The Transition from Two Phase Bubble Flow to Slug Flow," Report No. 7-7673-22, Department of Mechanical Engineering, M.I.T., June, 1962.

11. Wallis, G. B., "Some Hydrodynamic Aspects of Two Phase Flow and Boiling," International Heat Transfer Conference, Boulder, Colorado, 1961.
12. Haywood, R. W., G. A. Knight, M. A. Middleton, J. R. S. Thom, "Experimental Study of the Flow Conditions and Pressure Drop of Steam-Water Mixtures at High Pressures in Heated and Unheated Tubes," Presented at the Institution of Mechanical Engineers, London, England, p. 26 and p. 36, March 29, 1961.
13. Marchaterre, J. F., "Effect of Pressure on Boiling Density in Multiple Rectangular Channels," ANL 5522, February, 1956.
14. ANL 5511, Quarterly Progress Report, Section 11, July, Aug., Sept., 1955.
15. Spigt, C. L., J. P. Simon Thomas, M. Bogaardt, "Introductory Laboratory Studies of Boiling - Water Reactor Stability," Inst. of M.E. Two Phase Fluid Flow Symposium, London, England, 7 February 1962.
16. Egen, R. A., D. A. Dingee, J. W. Chastain, "Vapor Formation and Behavior in Boiling Heat Transfer," ASME Paper 57-A-74.
17. Stanley, D., "Wall Shear Stress in Two Phase Slug Flow," M.S. Thesis in Mechanical Engineering, M.I.T., June, 1962.
18. Hartnett, H. P., J. C. Y. Koh, S. T. McComas, "A Comparison of Predicted and Measured Friction Factors for Turbulent Flow Through Rectangular Ducts," Trans. A.S.M.E., J. of Heat Transfer, Vol. 84, Series C, No. 1, Aug. 1961.

LIST OF SYMBOLS

- A** Cross section area for flow
- D_b** Big channel section dimension, equal to pipe diameter for a pipe, large dimension for a rectangular cross section and shroud diameter for an annulus or tube bundle.
- D_c** Diameter of circle passing through the centers of the six tubes in the seven tube, tube bundle
- D_h** Four times flow area over wetted perimeter. The hydraulic diameter
- D_s** Small dimension equal to small dimension for a rectangle, insert diameter for an annulus and hydraulic diameter D_h for a tube bundle.
- D_t** Tube diameter for the tube bundle.
- K₁** Constant defined by the tube emptying experiment and equation (7).
- K₂** Constant depending on velocity profile and defined by equation (9).
It is assumed constant for Reynolds numbers bigger than 8000.
- K₃** Constant equal to 1.6 for heated channels and 1 for unheated.
- L** Channel length
Reynolds number based on through put velocity and liquid properties

$$- \left(\frac{Q_f + Q_g}{A} \right) \frac{\rho_f}{\mu_f}$$
It is the true Reynolds number of the liquid in the slug.
- Q_f** Liquid volume flow rate
- Q_g** Vapor volume flow rate
- R_g** Void fraction
- R_i** Annulus inner radius
- R_o** Annulus outer radius
- R_m** Annulus maximum velocity radius

- V Velocity
- V_b Bubble rise velocity with respect to the liquid ahead of the bubble.
- V_L Apparent liquid velocity defined by equation (4).
- V_g Apparent vapor velocity defined by equation (3).
- V_i Inlet velocity
- V_m Maximum velocity occurring at r_m
- V_{av} Average velocity
- x Distance from maximum velocity point to point in question
- x_m Distance from maximum velocity point to wall
- X Weight quality determined from a heat balance
- ρ Density
- ρ_L Liquid density
- ρ_g Vapor density
- ρ_i Inlet density
- τ_s Shroud shear stress
- τ_i Insert shear stress
- ν Kinematic viscosity

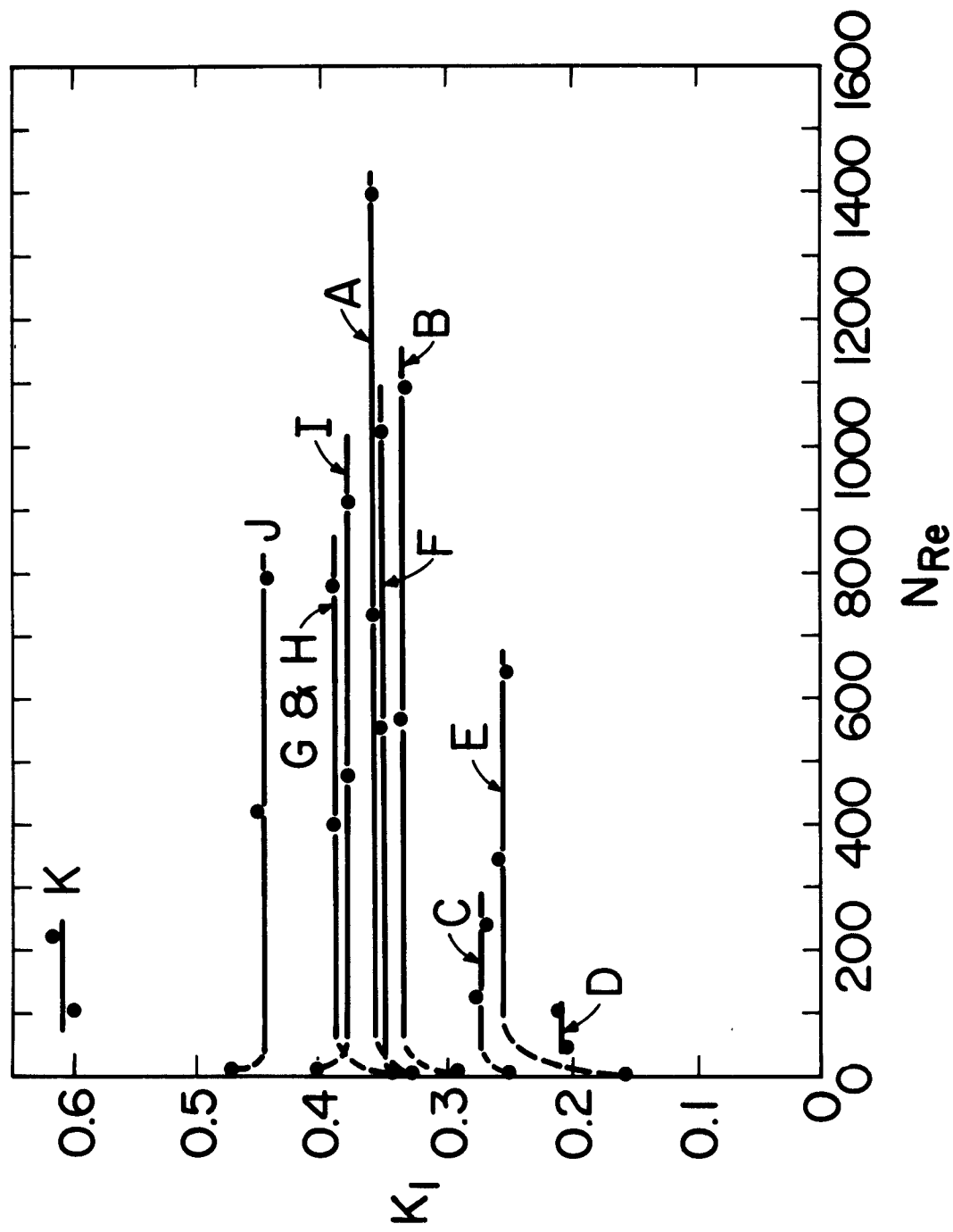


FIGURE 1

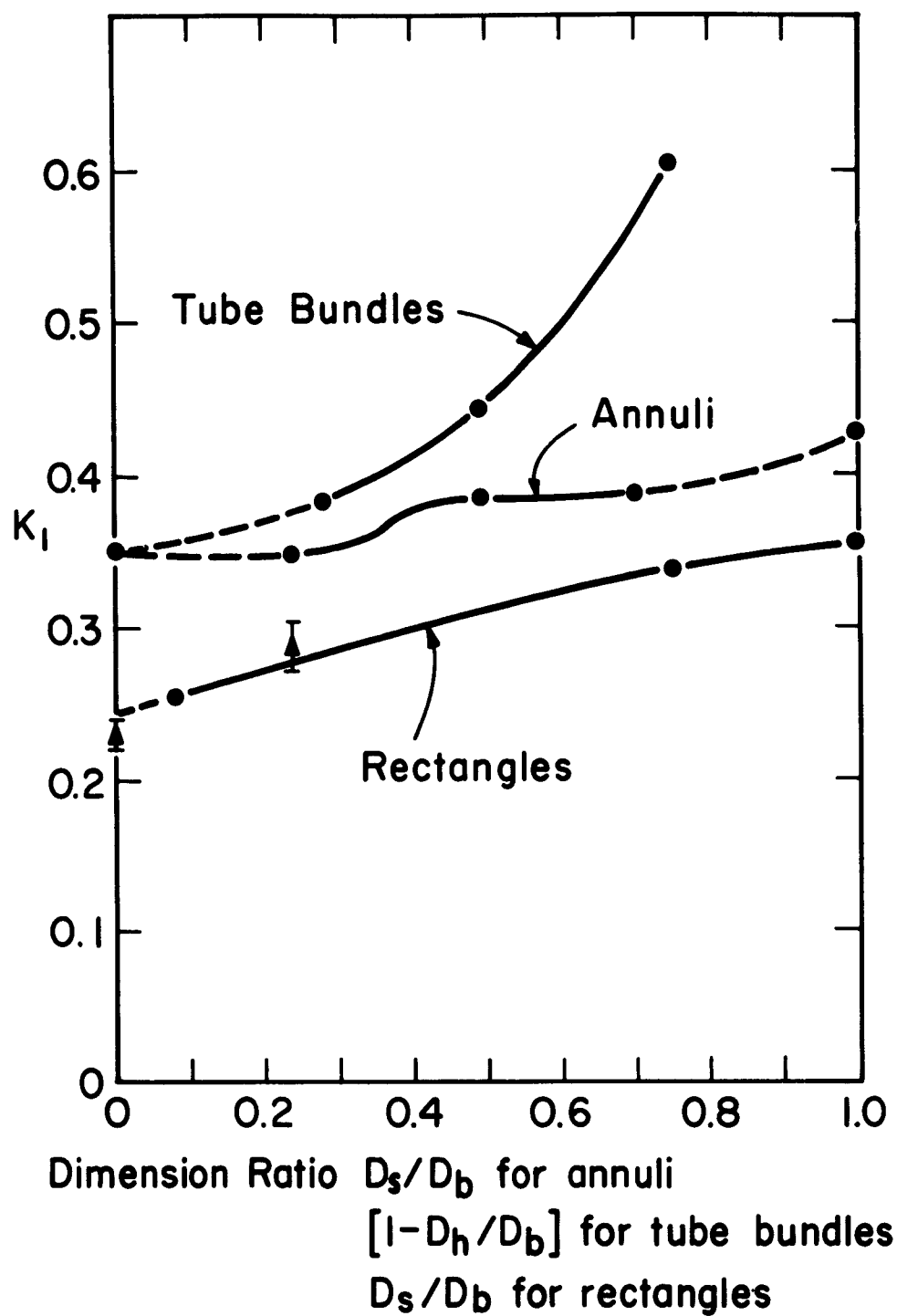
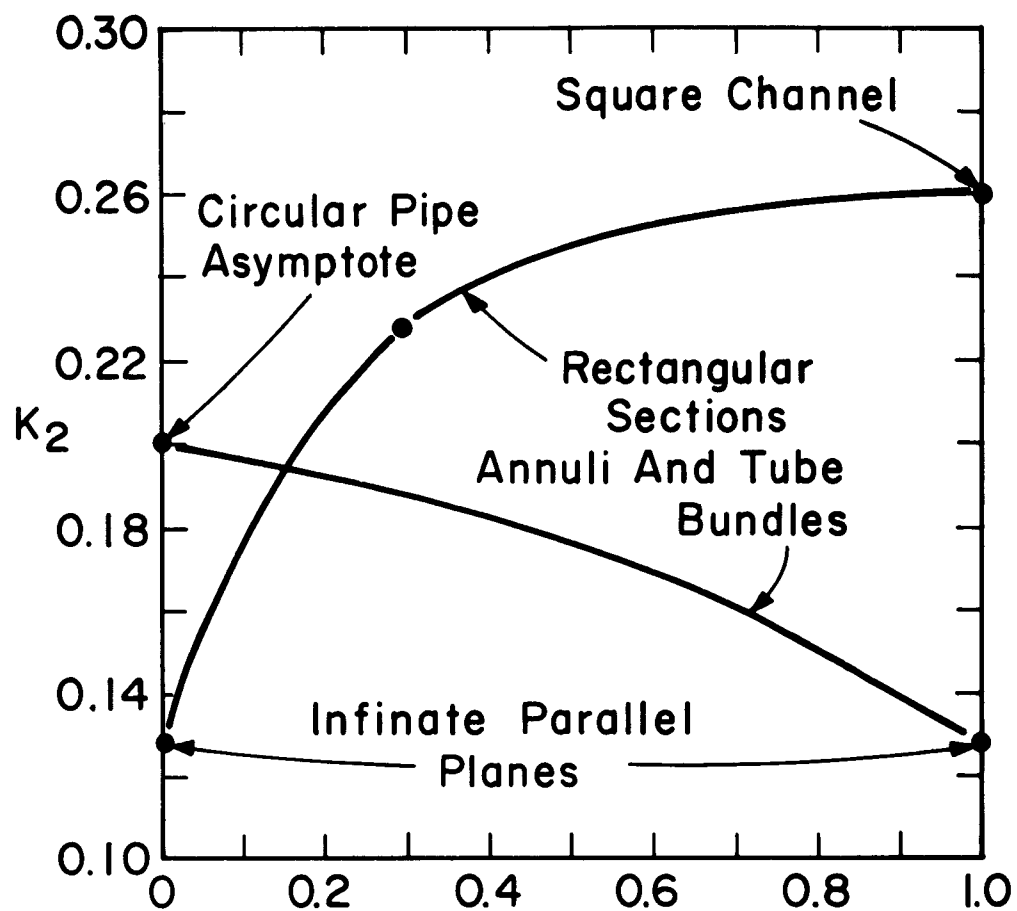


FIGURE 2



$\frac{D_s}{D_b}$ for Annuli

$\left(1 - \frac{D_h}{D_b}\right)$ for Tube Bundles

$\frac{D_s}{D_b}$ for Rectangles

FIGURE. 3

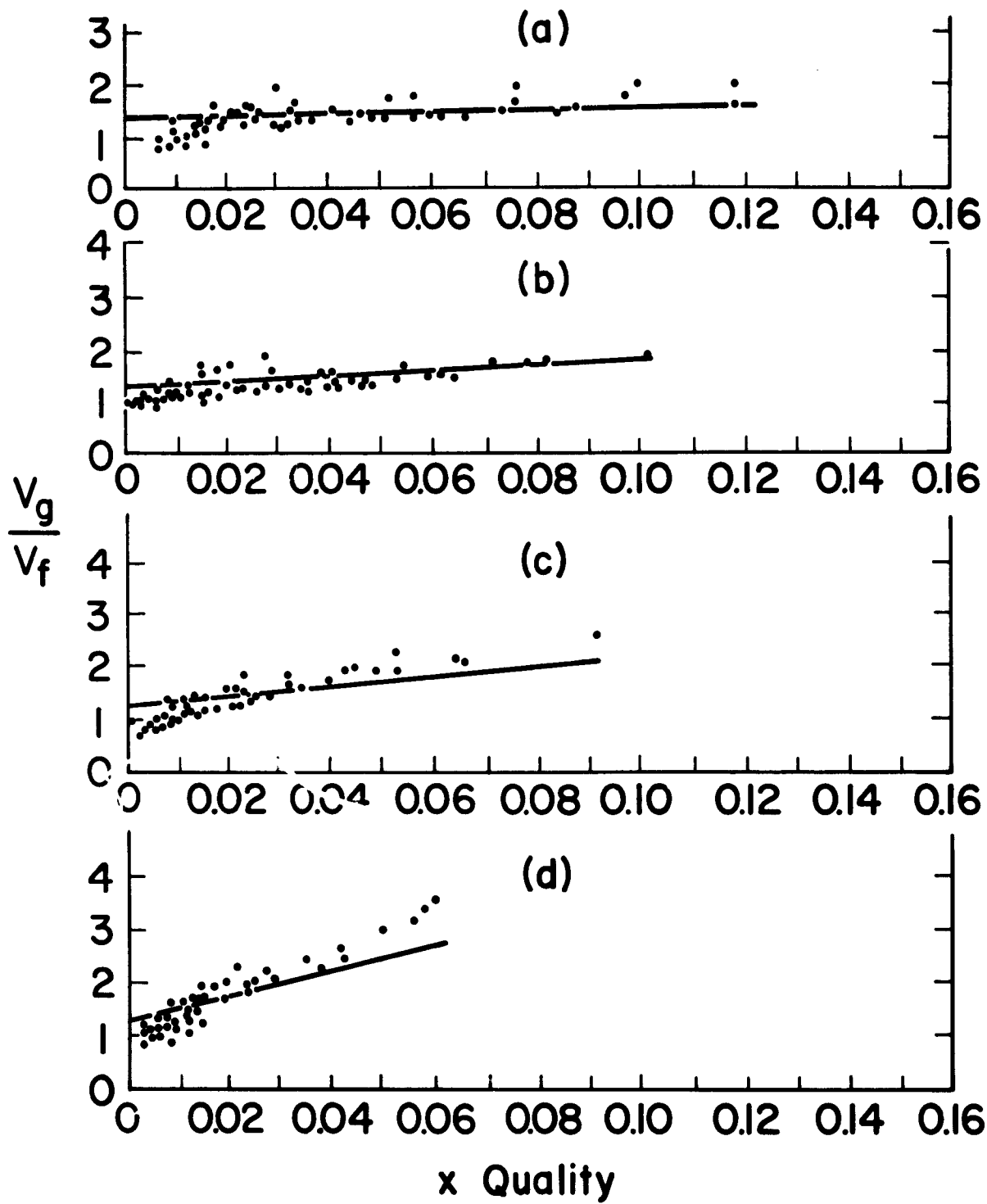


FIGURE 4

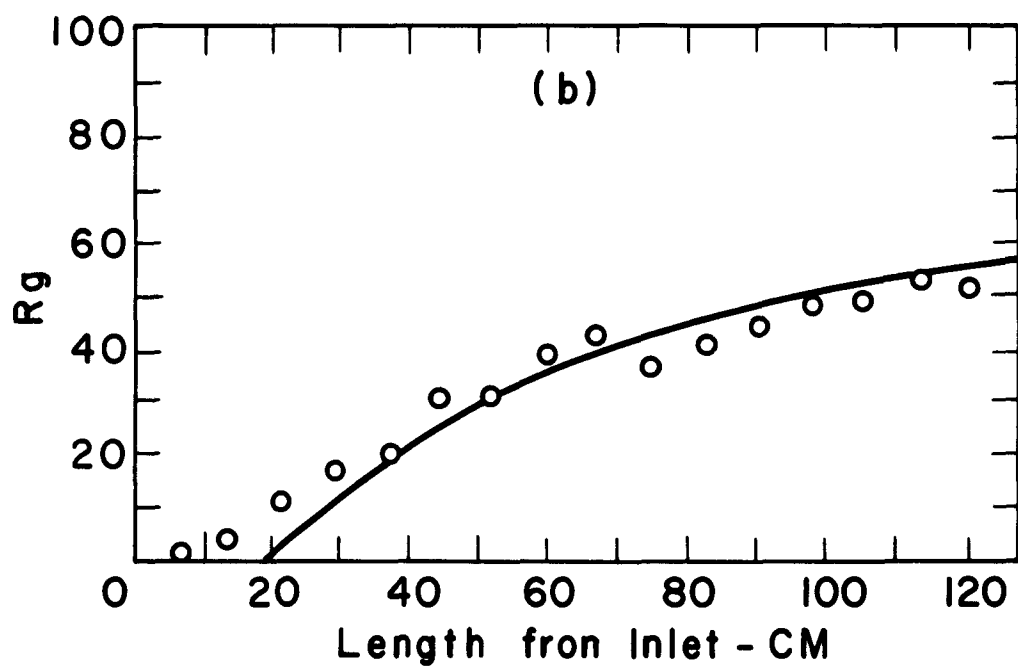
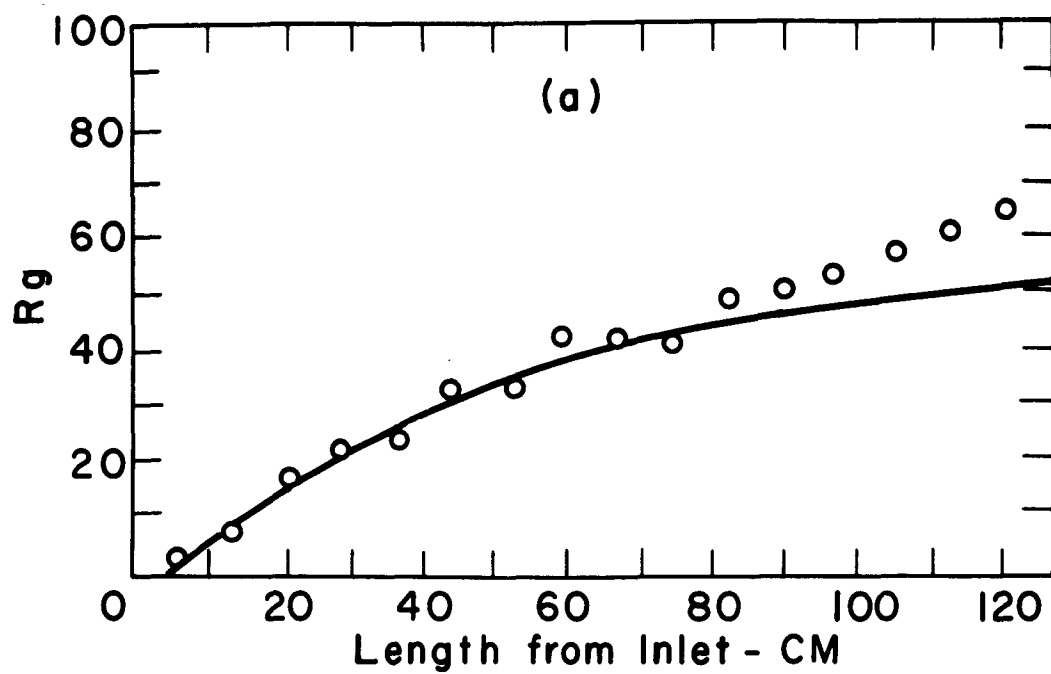


FIGURE 5

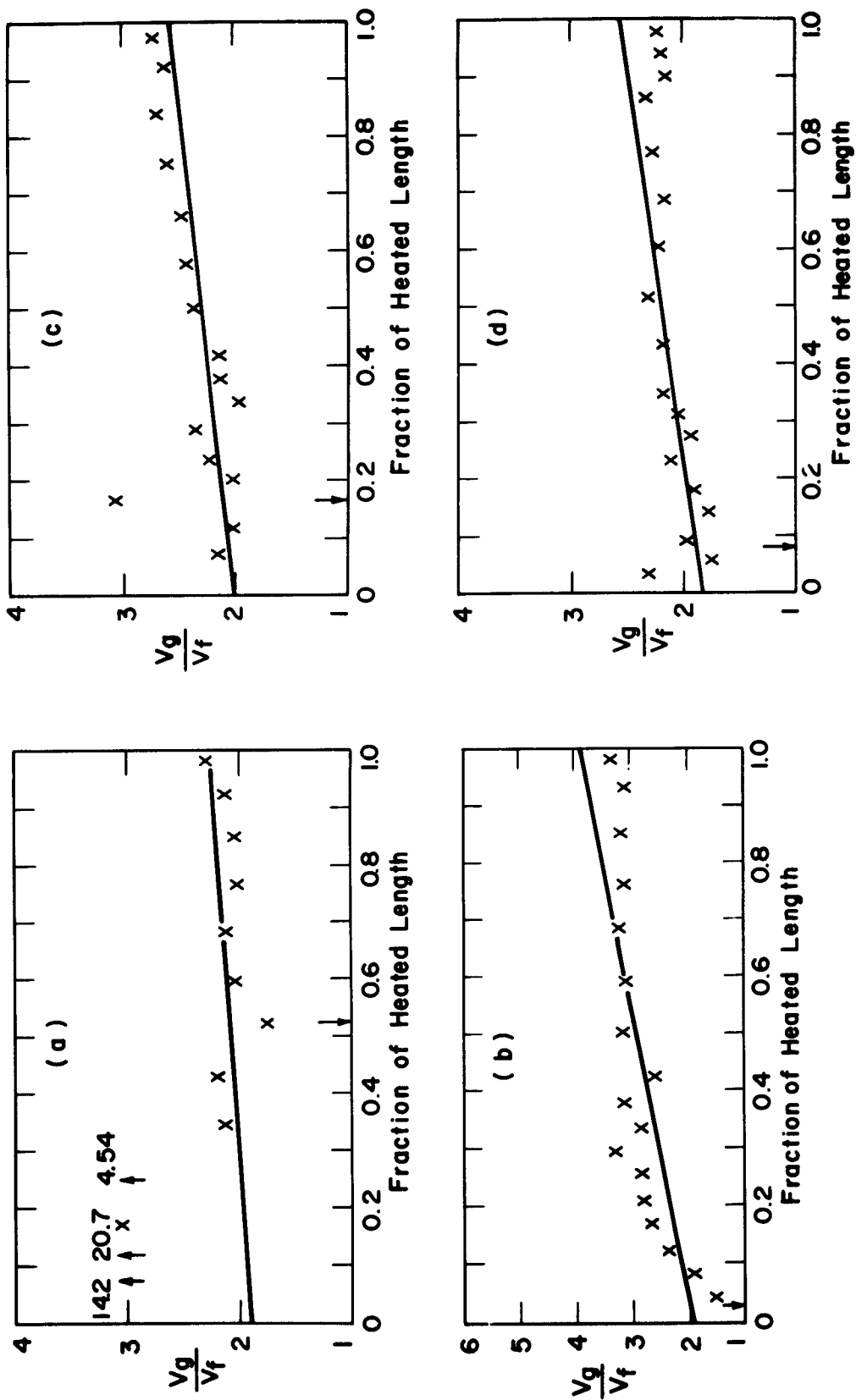


FIGURE 6

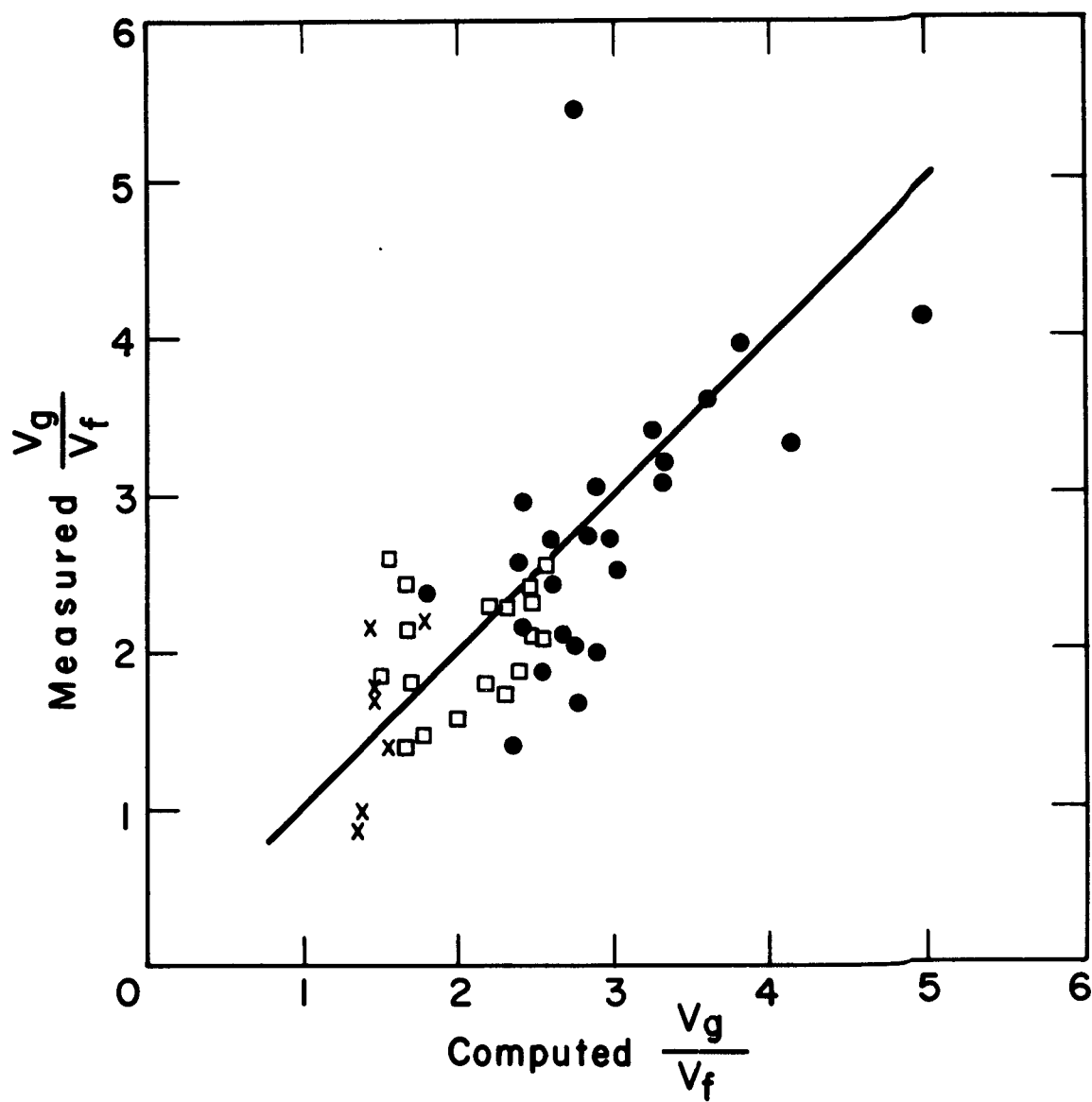
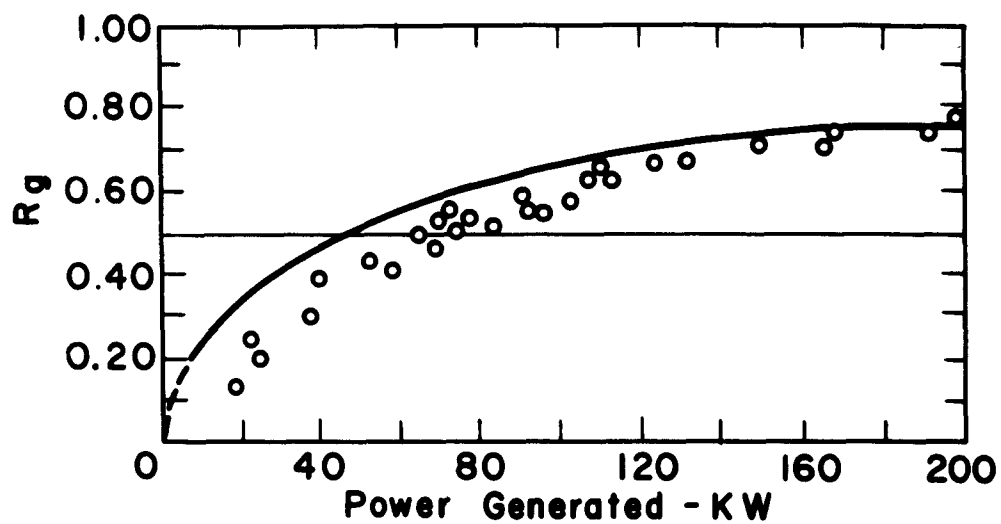
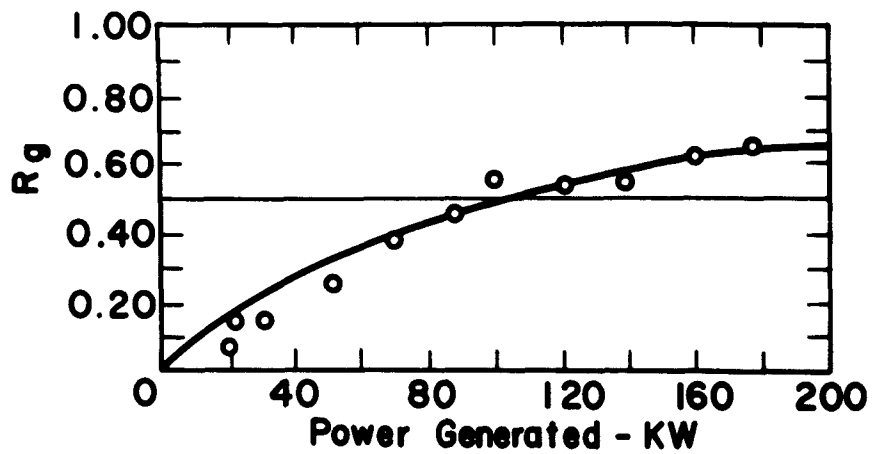


FIGURE 7



(a)



(b)

FIGURE 8